

# Inverted pendulum under hysteretic control: stability zones and periodic solutions

Mikhail E. Semenov · Darya V. Shevlyakova · Peter A. Meleshenko

Received: 30 April 2013 / Accepted: 2 September 2013 / Published online: 25 September 2013  
© Springer Science+Business Media Dordrecht 2013

**Abstract** In this paper, the mathematical model of the stabilization of the inverted pendulum with vertically oscillating suspension under hysteretic control is constructed. In the frame of the presented model, the stability criteria for the linearized equations of motion are found. We have made the numerical construction of the stability zones in the two-dimensional parameter space. Dependencies between initial conditions and driven parameters that provide periodic oscillations of the pendulum are obtained.

**Keywords** Inverted pendulum · Hysteretic control · Monodromy matrix · Stability zone · Periodic solutions

---

M.E. Semenov (✉)  
Meteorology Department, Zhukovsky–Gagarin Air Force Academy, Starykh Bolshevikov st. 54 “A”,  
394064 Voronezh, Russia  
e-mail: [mkl150@mail.ru](mailto:mkl150@mail.ru)

D.V. Shevlyakova  
Faculty of Computer Sciences, Voronezh State University,  
Universitetskaya sq. 1, 394006 Voronezh, Russia

P.A. Meleshenko  
Mathematics Department, Zhukovsky–Gagarin Air Force Academy, Starykh Bolshevikov st. 54 “A”,  
394064 Voronezh, Russia

*Present address:*

M.E. Semenov · P.A. Meleshenko  
Digital Technologies Department, Voronezh State University, Universitetskaya sq. 1, 394006 Voronezh, Russia

## 1 Introduction

The problem of the inverted pendulum has a long history [14, 15, 33] and remains relevant even in the present days [1, 5–7, 12, 20, 23, 26, 34, 35, 37]. As is well known, the model of the inverted pendulum plays the central role in the control theory [4, 5, 10, 13, 16, 22, 28, 34, 35]. It is a well established benchmark problem that provides many challenging problems to control design. Because of their nonlinear nature, pendulums have maintained their usefulness and they are now used to illustrate many of the ideas emerging in the field of nonlinear control [2]. Typical examples are feedback stabilization, variable structure control, passivity based control, back-stepping and forwarding, nonlinear observers, friction compensation, and nonlinear model reduction. The challenges of control made the inverted pendulum systems a classic tools in control laboratories.<sup>1</sup>

According to control purposes of the inverted pendulum, the control of inverted pendulum can be divided into three aspects. The first aspect that is widely researched is the swing-up control of inverted pendu-

---

<sup>1</sup> Here, it should be noted that although a lot of control algorithm are researched in the systems control design, PID controller is the most widely used controller structure in the realization of a control system [34]. The advantages of the PID controller, which have greatly contributed to its wide acceptance, are its simplicity and sufficient ability to solve many practical control problems.

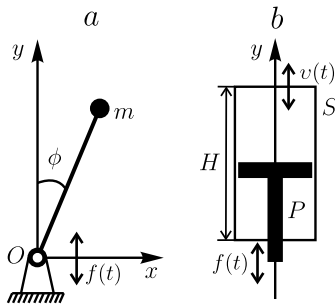


**Fig. 1** Geometry of the problem. Panel **a**: general view of the inverted pendulum. Panel **b**: the suspension point (cylinder and piston)

lum [10, 22, 28].<sup>2</sup> The interesting and important results on the time optimal control of the inverted pendulum were obtained in [10, 28]. In particular, in [28] the optimal transients (taking into account the cylindrical character of the states space of the system under control) were built for different values of the parameters and constraints on the control torque. The second aspect is the stabilization of the inverted pendulum [3, 9]. The third aspect is the tracking control of the inverted pendulum [8]. In practice, stabilization and tracking control are more useful for application.

Also, the model of the inverted pendulum (especially, under various kinds of control of the motion of the suspension point) is widely used in the various fields of physics [31], applied mathematics [35], engineer sciences [19, 32], neuroscience [36], economics [30], and others.

The model of an inverted pendulum with an oscillating suspension point (see panel a in Fig. 1) was studied in detail by Kapitza [14, 15]. Let us recall that the equation of motion of pendulum has the form:

$$\ddot{\phi} - \frac{1}{l}[g + \ddot{f}(t)] \sin \phi = 0 \quad (1)$$

where  $\phi$  is the angle of vertical deviation of the pendulum,  $l$  is the pendulum's length,  $g$  is the gravitational acceleration, and  $f(t)$  is the law of motion of the suspension point (of course, this equation should

<sup>2</sup>The one-dimensional swinging inverted pendulum with two degrees of freedom is a popular demonstration of using feedback control to stabilize an open-loop unstable system. Since the system is inherently nonlinear, it has been used extensively by the control engineers to verify a modern control theory. In this system, an inverted pendulum is attached to a cart equipped with a motor that drives it along a horizontal track [11].

be considered together with the corresponding initial conditions).

As is known, if the motion of the suspension point is of harmonic character, then Eq. (1) reduces to the Mathieu equation, studied in detail, e.g., in [21].

In order to make an adequate description of the dynamics of real physical and mechanical systems, it is necessary to take into account the effects of hysteretic nature such as “backlash,” “stops,” etc. [25]. The mathematical models of such nonlinearities according to the classical patterns of Krasnosel'skii and Pokrovskii [18], reduce to operators that are treated as converters in appropriate function spaces. The dynamics of such converters are described by the relation of “input-state” and “state-output.”

As is known, most of the real physical and technical systems contain a various kind of parts that can be represented as a cylinder with a piston [25]. Inevitably, the backlashes appear in such systems during its long operation due to the “aging” of the materials. As was mentioned above, such backlashes are of hysteretic nature and the analysis of such nonlinearities is quite important and an actual problem. In this paper, we investigate the problem of the inverted pendulum under hysteretic control in the form of backlash. More specific, we investigate the dynamical features of such a system depending on the control parameters, especially on the cylinder's length that of hysteretic nature. Let us note also that the system under consideration can be considered as a successful model for a real mechanical system with a hysteretic type of nonlinearity.

The paper is organized as follows. In Sect. 2, we construct the mathematical model of the inverted pendulum under hysteretic control. Section 3 is dedicated to the problem of stability of the linearized equation of motion. Particularly, in this section the monodromy matrix and the stability condition for the inverted pendulum under hysteretic control are found in the explicit analytical form. In Sect. 4, the stability zones of the presented system are analyzed in detail. Section 5 is dedicated to the analysis of the periodic solutions for the system under consideration taking into account that the hysteretic control takes place. In the last section, all the main results of this paper are summarized.

## 2 Mathematical model

Let us consider a system where the base of the pendulum is a physical system ( $P, S$ ) formed by a cylinder

of length  $H$  and the piston  $P$ .<sup>3</sup> Both the cylinder and piston can move in the direction of the vertical axis as it is shown in panel b of the Fig. 1.

We determine the piston’s position by the coordinate  $f(t)$  and the cylinder’s position by coordinate  $v(t)$ . Let us assume also that the “leading” element in the system  $(P, S)$  is a cylinder  $P$ . In this assumption, the system  $(P, S)$  can be considered as a converter  $\Gamma$  with the input signal  $f(t)$  (piston’s position) and the output signal  $v(t)$  (cylinder’s position). Such a converter is called *backlash*. The set of its possible states is  $f(t) \leq v(t) \leq f(t) + H$  ( $-\infty < f(t) < \infty$ ). The cylinder’s position  $v(t)$  at  $t > t_0$  is defined by  $v(t) = \Gamma[t_0, v(t_0)]f(t)$ , where  $\Gamma[t_0, v(t_0)]$  is the operator defined for each  $v_0 = v(t_0)$  on the set of continuous inputs  $f(t)$  ( $t > t_0$ ) for which  $v_0 - H < f(t) < v_0$  [18].

We assume that the piston’s acceleration periodically changes from  $-a\omega^2$  to  $a\omega^2$  with the frequency  $\omega$ . This assumption consists in the fact that the linearized equation of motion of such a pendulum can be written in the form:<sup>4</sup>

$$\begin{aligned} \ddot{\phi} - \frac{1}{l}[g + a\omega^2 G(t, H)w(t)]\phi &= 0, \\ w(t) &= -\text{sign}[\sin(\omega t)], \\ \phi(0) = \phi_{10}, \quad \dot{\phi}(0) &= \phi_{20}, \end{aligned} \tag{2}$$

where  $\text{sign}(z)$  is the usual signum function,  $G(t, H)w(t)$  is the acceleration of the suspension point and

$$G(t, H) = \begin{cases} 0, & t \in (t^*, t^* + \Delta t), \\ 1, & t \text{ out of } (t^*, t^* + \Delta t), \end{cases}$$

where  $t^*$  are the moments after which the acceleration’s sign change takes place;  $\Delta t = \sqrt{\frac{2H}{a\omega^2}}$  is the time for which the piston passes through the cylinder.

<sup>3</sup>Here, we would like to note that both the cylinder and piston are ideal, absolutely rigid, and can move along the  $y$ -axis in the infinite ranges.

<sup>4</sup>It should also be pointed out that such a periodic behavior of the piston’s acceleration (namely, the fact that the acceleration of the piston changes from  $-a\omega^2$  to  $a\omega^2$ ) is an assumption of the model presented in this paper. Such a model allows us to obtain some analytical results (the explicit conditions for the stability zones). Also, the numerical simulations are most effectively in the frame of this model. Moreover, such a model of the piston’s behavior most effectively and adequately describes the dynamics of the parts of real technical devices.

### 3 Stability of linearized equation

Let us pass to dimensionless units in (2) using the following change:

$$\begin{aligned} x &\equiv \phi, \quad \tau = \omega t, \quad k = \frac{g}{l\omega^2}, \quad s = \frac{a}{l}, \\ \Delta\tau &= \sqrt{\frac{2H}{sl}}. \end{aligned}$$

As a result, we obtain an equation similar to the Meissner equation [21], but with the negative coefficients and hysteretic nonlinearity, namely:

$$\begin{aligned} \ddot{x} - [k - sG(\tau, H) \text{sign}(\sin \tau)]x &= 0, \\ G(\tau, H) &= \begin{cases} 0, & \tau \in (\tau^*, \tau^* + \Delta\tau), \\ 1, & \tau \text{ out of } (\tau^*, \tau^* + \Delta\tau), \end{cases} \end{aligned} \tag{3}$$

$$x(0) = x_{10}, \quad \dot{x}(0) = x_{20}.$$

We can write Eq. (3) in the form of an equivalent system:

$$\begin{aligned} \begin{cases} \dot{x}_1 = x_2, \\ \dot{x}_2 = p(\tau)x_1, \end{cases} \\ x_1(0) = x_{10}, \quad x_2(0) = x_{20}. \end{aligned} \tag{4}$$

The matrix of this system has the form:

$$\mathbf{P}(\tau) = \begin{pmatrix} 0 & 1 \\ p(\tau) & 0 \end{pmatrix},$$

where  $p(\tau) = k - sG(\tau, H) \text{sign}(\sin \tau)$ . In the frame of our assumptions, the matrix  $\mathbf{P}(\tau)$  is a periodic function of time with the period  $2\pi$ , namely:  $\mathbf{P}(\tau + 2\pi) \equiv \mathbf{P}(\tau)$ .

Let us say that Eq. (3) is stable (or unstable) according to Lagrange if the system (4) is stable (or unstable, respectively). It means that all solutions  $x(\tau)$  of the stable Eq. (3) are bounded in  $[\tau_0, \infty)$  together with the derivatives  $\dot{x}(\tau)$ .

Following the results of Floquet [27], the investigation of the stability of such systems reduces to the problem of finding of the fundamental matrix of the solutions at the moment  $2\pi$  (the so-called *monodromy matrix*) and evaluation of its eigenvalues (the so-called *multipliers*). For the stability of the periodic system, it is necessary and sufficient that the following condition takes place  $|\varrho| < 1$  (all the multipliers are placed inside the unit circle).

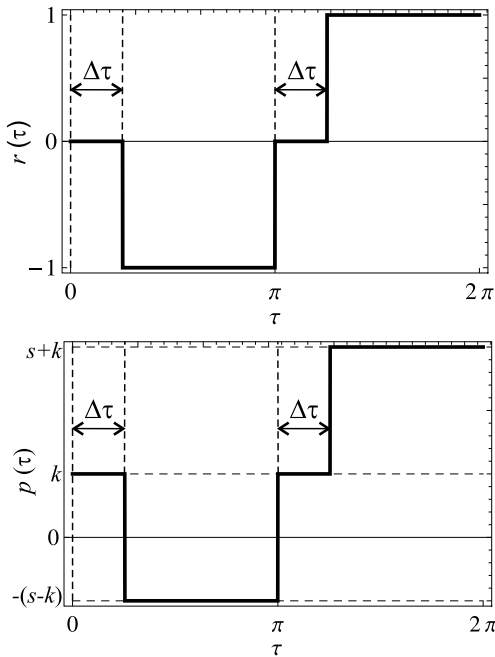


**Fig. 2** Functions  $r(\tau)$  and  $p(\tau)$

Due to the fact that the matrix  $\mathbf{P}(\tau)$  is a piecewise-constant, the fundamental system of solutions and the monodromy matrix can be constructed in the closed form. In order to do this, let us consider behavior of a piecewise-constant function  $r(\tau) =$

$-G(\tau, H) \text{sign}(\sin \tau)$  with the period  $2\pi$ , and a function  $p(\tau)$ , respectively (see Fig. 2).

As we see from Fig. 2, in the interval  $(0, 2\pi)$  the system (4) can be described by the following linear systems with the constant coefficients:

$$\begin{cases} \dot{x}_1^1 = x_2^1, \\ \dot{x}_2^1 = kx_1^1, \end{cases} \quad \tau \in [0, \Delta\tau], \tag{5}$$

$$\begin{cases} \dot{x}_1^2 = x_2^2, \\ \dot{x}_2^2 = -(s-k)x_1^2, \end{cases} \quad \tau \in [\Delta\tau, \pi], \tag{6}$$

$$\begin{cases} \dot{x}_1^3 = x_2^3, \\ \dot{x}_2^3 = kx_1^3, \end{cases} \quad \tau \in [\pi, \pi + \Delta\tau], \tag{7}$$

$$\begin{cases} \dot{x}_1^4 = x_2^4, \\ \dot{x}_2^4 = (k+s)x_1^4, \end{cases} \quad \tau \in [\pi + \Delta\tau, 2\pi]. \tag{8}$$

Since the fundamental matrix should be continuous, the solutions of (5)–(8) should match at the corresponding points, namely:

$$\mathbf{X}^1(0) = \mathbf{E}, \quad \mathbf{X}^j(\tau_j^*) = \mathbf{X}^{j+1}(\tau_j^*),$$

where  $i = 1, 2, 3$ ,  $\tau_i^*$  are the moments at which the control changes during the period,  $\mathbf{E}$  is the unity matrix.

Consistent integration of the systems (5)–(8) leads to the following fundamental matrices:

$$\mathbf{X}^1(\tau) = \begin{pmatrix} \cosh(\sqrt{k}\tau) & \frac{1}{\sqrt{k}} \sinh(\sqrt{k}\tau) \\ \sqrt{k} \sinh(\sqrt{k}\tau) & \cosh(\sqrt{k}\tau) \end{pmatrix},$$

$$\mathbf{X}^2(\tau) = \mathbf{X}^1(\Delta\tau) \begin{pmatrix} \cos[k_2(\tau - \Delta\tau)] & \frac{1}{k_2} \sin[k_2(\tau - \Delta\tau)] \\ -k_2 \sin[k_2(\tau - \Delta\tau)] & \cos[k_2(\tau - \Delta\tau)] \end{pmatrix},$$

$$\mathbf{X}^3(\tau) = \mathbf{X}^2(\pi) \begin{pmatrix} \cosh[\sqrt{k}(\tau - \pi)] & \frac{1}{\sqrt{k}} \sinh[\sqrt{k}(\tau - \pi)] \\ \sqrt{k} \sinh[\sqrt{k}(\tau - \pi)] & \cosh[\sqrt{k}(\tau - \pi)] \end{pmatrix},$$

$$\mathbf{X}^4(\tau) = \mathbf{X}^3(\pi + \Delta\tau) \begin{pmatrix} \cosh[k_1(\tau - \pi - \Delta\tau)] & \frac{1}{k_1} \sinh[k_1(\tau - \pi - \Delta\tau)] \\ k_1 \sinh[k_1(\tau - \pi - \Delta\tau)] & \cosh[k_1(\tau - \pi - \Delta\tau)] \end{pmatrix}.$$

Putting  $\tau = 2\pi$  in  $\mathbf{X}^4(\tau)$ , we obtain the following form of the monodromy matrix of the system (4):

$$\begin{aligned} \mathbf{A} &= \mathbf{X}(2\pi) \\ &= \begin{pmatrix} \cosh(\sqrt{k}\Delta\tau) & \frac{1}{\sqrt{k}} \sinh(\sqrt{k}\Delta\tau) \\ \sqrt{k} \sinh(\sqrt{k}\Delta\tau) & \cosh(\sqrt{k}\Delta\tau) \end{pmatrix} \end{aligned}$$

$$\begin{aligned} &\times \begin{pmatrix} \cos(k_2\gamma) & \frac{1}{k_2} \sin(k_2\gamma) \\ -k_2 \sin(k_2\gamma) & \cos(k_2\gamma) \end{pmatrix} \\ &\times \begin{pmatrix} \cosh(\sqrt{k}\Delta\tau) & \frac{1}{\sqrt{k}} \sinh(\sqrt{k}\Delta\tau) \\ \sqrt{k} \sinh(\sqrt{k}\Delta\tau) & \cosh(\sqrt{k}\Delta\tau) \end{pmatrix} \\ &\times \begin{pmatrix} \cosh(k_1\gamma) & \frac{1}{k_1} \sinh(k_1\gamma) \\ k_1 \sinh(k_1\gamma) & \cosh(k_1\gamma) \end{pmatrix}, \end{aligned} \tag{9}$$

where  $(k_1)^2 = k + s$ ,  $(k_2)^2 = s - k$  ( $s > k$ ),  $\gamma = \pi - \Delta\tau$ . Let us write also the characteristic equation for the matrix  $\mathbf{A}$ :

$$\|\mathbf{A} - \varrho\mathbf{E}\| = \begin{vmatrix} a_{11} - \varrho & a_{12} \\ a_{21} & a_{22} - \varrho \end{vmatrix} = \varrho^2 + \alpha\varrho + \beta = 0, \tag{10}$$

where

$$\beta = (-1)^2 \exp\left(\int_0^T \text{Sp}[\mathbf{P}(\tau)] d\tau\right) = 1$$

[24] and  $\alpha = -(a_{11} + a_{22})$ .

The product of the roots  $\varrho_1$  and  $\varrho_2$  of Eq. (10) is equal to unity, so the motion will be stable at  $|\alpha| < 2$  only, i.e., when the modules both of multipliers are equal to unity, but these multipliers are different. Thus, we obtain the following condition for the stability of solutions of (3):

$$|a_{11} + a_{22}| < 2. \tag{11}$$

Using (9) the condition (11) can be written in the explicit form:

$$\begin{aligned} & \left| \cos(k_2\gamma) \left[ 2 \cosh(2\sqrt{k}\Delta\tau) \cosh(k_1\gamma) \right. \right. \\ & \quad \left. \left. + \sinh(2\sqrt{k}\Delta\tau) \sinh(k_1\gamma) \left( \frac{\sqrt{k}}{k_1} + \frac{k_1}{\sqrt{k}} \right) \right] \right. \\ & \quad \left. + \sin(k_2\gamma) \left[ \sinh(2\sqrt{k}\Delta\tau) \cosh(k_1\gamma) \left( \frac{\sqrt{k}}{k_2} - \frac{k_2}{\sqrt{k}} \right) \right. \right. \\ & \quad \left. \left. + \cosh^2(\sqrt{k}\Delta\tau) \sinh(k_1\gamma) \left( \frac{k_1}{k_2} - \frac{k_2}{k_1} \right) \right. \right. \\ & \quad \left. \left. + \sinh^2(\sqrt{k}\Delta\tau) \sinh(k_1\gamma) \left( \frac{k}{k_1k_2} - \frac{k_1k_2}{k} \right) \right] \right| < 2. \tag{12} \end{aligned}$$

Thus, the *stability zone* of the system (4) in the space of parameters is defined by the inequality (12).

### 4 Stability zones

Let us consider Eq. (3) at  $H = 0$ , i.e., in the absence of the hysteretic nonlinearity:

$$\ddot{x} - [k - s \cdot \text{sign}(\sin \tau)]x = 0, \tag{13}$$

then  $\Delta\tau = 0$  and the inequality (12) takes the form:

$$\begin{aligned} & \left| \cosh(\pi k_1) \cos(\pi k_2) \right. \\ & \quad \left. + \frac{1}{2} \left( \frac{k_1}{k_2} - \frac{k_2}{k_1} \right) \sinh(\pi k_1) \sin(\pi k_2) \right| < 1. \tag{14} \end{aligned}$$

Now we construct numerically a solution of (14) with relation to the parameters  $k$  and  $s$  (see the panel a in Fig. 3). In panel b of the Fig. 3 we show also the stability zone for the Meissner equation obtained by Sato [29].

As we can see, these diagrams are the mirror images of each other because of opposite signs at  $x$  in the corresponding equations.

Let us construct the stability zone for the system (9). Such a system has a three-dimensional parameter space because of dependence on the three parameters takes place (namely, the dimensionless variables  $k$ ,  $s$ , and the piston’s length  $H$ ). We set the length of the pendulum as  $l = 1$  m.

Figure 4 shows that the stability zones do not qualitatively change, but only slightly deformed with growth of  $H$ . Note that in the presented problem the parameters  $k$  and  $s$  can take the positive values only. The change of the stability zone in the positive half-plane is shown in Fig. 5. Also, in this figure, we see that the growth of the parameter  $H$  leads to the increasing of the lower boundary of the stability zone. Moreover, we see in this figure that with increasing of the hysteretic parameter (see the panel f) the boundaries of the stability zones become multivalued functions (namely, the function  $s(k)$ ). Such a behavior of the boundaries is connected with the fact that the main equation of the model contains the hysteretic nonlinearity (hysteretic behavior of the control parameter  $H$ ).

Stability zones in the space of parameters of the system (see Eq. (2)) are shown in Fig. 6. This figure shows that the area of stability zone essentially unchanged with increasing of the length of piston  $H$ , just only shifted (for the values of  $H$  in the interval  $H \in [0, 0.5]$ ). This means that for any  $H$  in the presented interval there exists a pair of values  $\omega$  and  $a$  to ensure the stability of the vertical position of the inverted pendulum with oscillating suspension and the hysteretic nonlinearity. However, as we can see in panel f, at  $H = 1$ , there are two domains of values  $\omega$  and  $a$  that ensure the stability of the vertical position.

**Fig. 3** Stability zones in the absence of the hysteretic control ( $H = 0$ ): panel **a** corresponds to Eq. (13); panel **b** corresponds to the Meissner equation

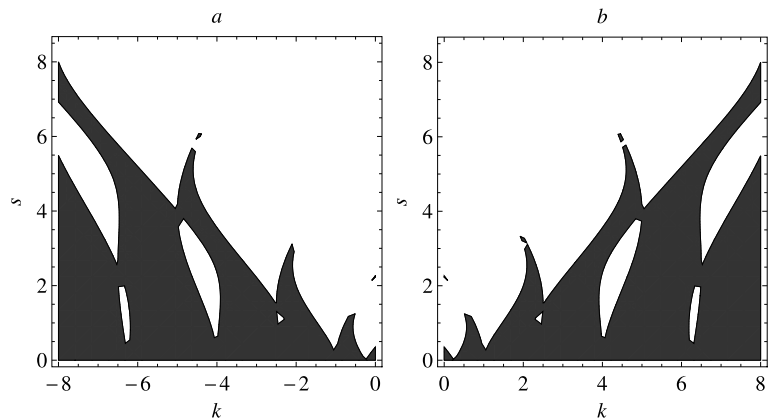
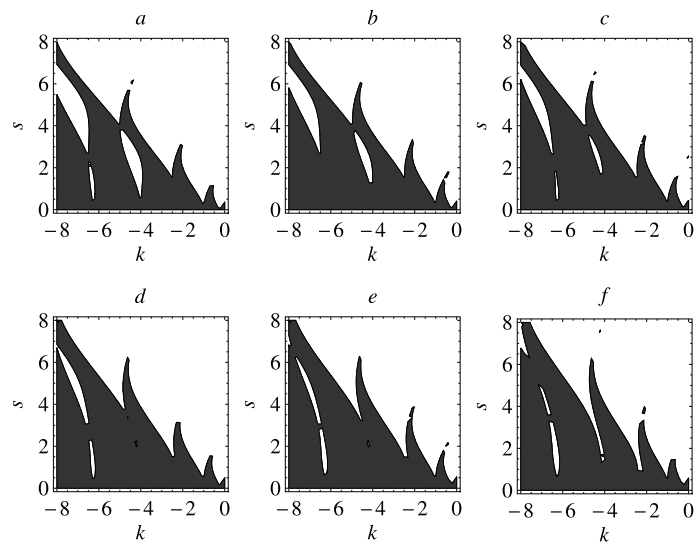


**Fig. 4** Stability zones in the presence of the hysteretic control. Panel **a** is  $H = 0$  m, panel **b** is  $H = 0.2$  m, panel **c** is  $H = 0.4$  m, panel **d** is  $H = 0.6$  m, panel **e** is  $H = 0.8$  m, panel **f** is  $H = 1$  m



It should also be pointed out that in full analogy with Fig. 5 the boundaries of the stability zones become multivalued functions (in this case, the function  $\omega(a)$ ) when the hysteretic parameter  $H$  increases. Such a behavior of the boundaries follows from the fact that in the presence of the hysteretic control the main equation (2) (together with the corresponding monodromy matrix (9)) becomes essentially nonlinear.

In Fig. 7, we plot the dependencies of the oscillation frequency (namely, the frequency which lies on the border of the stability zone, in other words, the frequency which ensuring the stability of solutions of (2)), on the length of the piston  $H$  at different values of  $a$  (oscillation amplitude for the piston).

Let us note that the parameters which satisfy the inequality (12) correspond to the almost periodic oscillations [17] relative to the top of the pendulum. In

order to confirm these results, we present the plots of characteristics of oscillations (in the linearized model described by Eq. (2)) of the inverted pendulum with length  $l = 1$  m and hysteretic nonlinearity  $H = 0.05$  m (Fig. 8). The amplitude and frequency of oscillation of the piston are  $a = 0.15$  m and  $\omega = 30$  s<sup>-1</sup>, respectively. The initial conditions are  $\phi(0) = 0.2$  and  $\dot{\phi}(0) = 1$  s<sup>-1</sup>.

## 5 Periodic solutions

Now, let us consider the behavior of the pendulum on the edges of the stability zone. In the characteristic equation for the monodromy matrix (10) such a situation corresponds to the two cases:  $\alpha = -2$  (left edge) and  $\alpha = 2$  (right edge). The multipliers in this case

**Fig. 5** Stability zones in the positive half-plane ( $k > 0, s > 0$ ) in the presence of the hysteretic control. Panel **a** is  $H = 0$  m, panel **b** is  $H = 0.2$  m, panel **c** is  $H = 0.4$  m, panel **d** is  $H = 0.6$  m, panel **e** is  $H = 0.8$  m, panel **f** is  $H = 1$  m

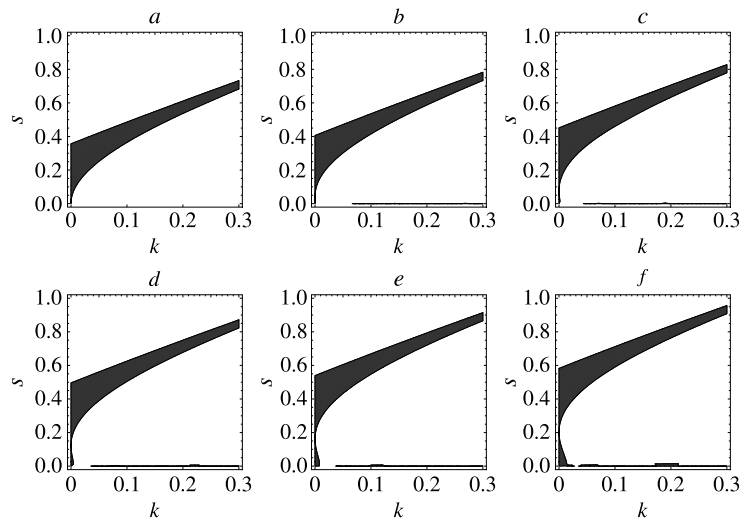
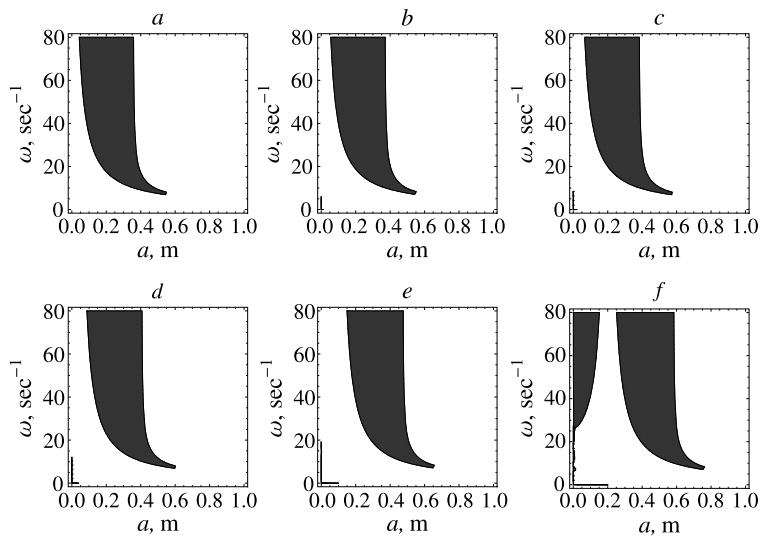


**Fig. 6** Stability zones in the coordinates  $a$  and  $\omega$  for different values of the parameter  $H$ . Panel **a** is  $H = 0$  m, panel **b** is  $H = 0.05$  m, panel **c** is  $H = 0.1$  m, panel **d** is  $H = 0.2$  m, panel **e** is  $H = 0.5$  m, panel **f** is  $H = 1$  m



have taken the values  $\varrho_1 = \varrho_2 = 1$  and  $\varrho_1 = \varrho_2 = -1$ , respectively.

If  $\varrho_1 = \varrho_2 = 1$ , then the corresponding normal solution will satisfy the equality  $\mathbf{X}(t + 2\pi) = \mathbf{X}(t)$ . Therefore, Eq. (2) has a periodic solution and the period of such a solution coincides with the period of the coefficients  $T_1 = \frac{2\pi}{\omega}$ .

In the second case ( $\varrho_1 = \varrho_2 = -1$ ), the corresponding normal solution will satisfy the equality  $\mathbf{X}(t + 2\pi) = -\mathbf{X}(t)$  (through the one more period  $\mathbf{X}(t + 4\pi) = -\mathbf{X}(t + 2\pi) = \mathbf{X}(t)$ ). This fact means that in the case when the multipliers equal to  $-1$ , Eq. (2) has a periodic solution with the period  $T_2 = \frac{4\pi}{\omega}$ .

The solutions are periodic (and hence limited) in both of the presented cases. We will say that they are stable by Lagrange. We assume also that all of the pendulum's parameters (in periodic regime of oscillations) should satisfy the following condition:

$$a_{11} + a_{22} = 2, \quad \text{for the period } T_1, \tag{15}$$

$$a_{11} + a_{22} = -2, \quad \text{for the period } T_2. \tag{16}$$

However, these conditions are necessary only, but not sufficient due to the fact that not for all of the nonzero initial values (for a given control with the parameters which satisfy to one of these equations) the periodic solutions will exist.

Note also that for the presented control described by the function  $v(t) = -a\omega^2 G(t, H) \text{sign}[\sin(\omega t)]$  the initial conditions lie in the first and third quadrants.

Put the following initial condition  $(\phi_{10}, \phi_{20})$ , and consider the case of periodic oscillations with the period  $T_1$ . In this case, the equality  $\mathbf{X}(0 + T_1) = \mathbf{A}\mathbf{X}(0) = \mathbf{X}(0)$  takes place, and also

$$\begin{pmatrix} a_{11} & a_{12} \\ a_{21} & a_{22} \end{pmatrix} \begin{pmatrix} \phi_{10} \\ \phi_{20} \end{pmatrix} = \begin{pmatrix} \phi_{10} \\ \phi_{20} \end{pmatrix}. \tag{17}$$

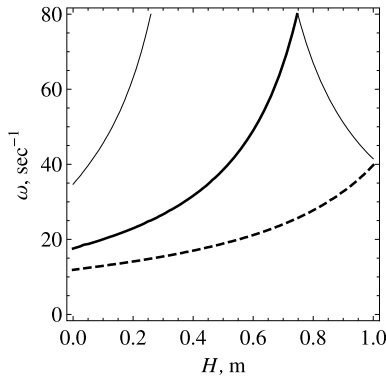
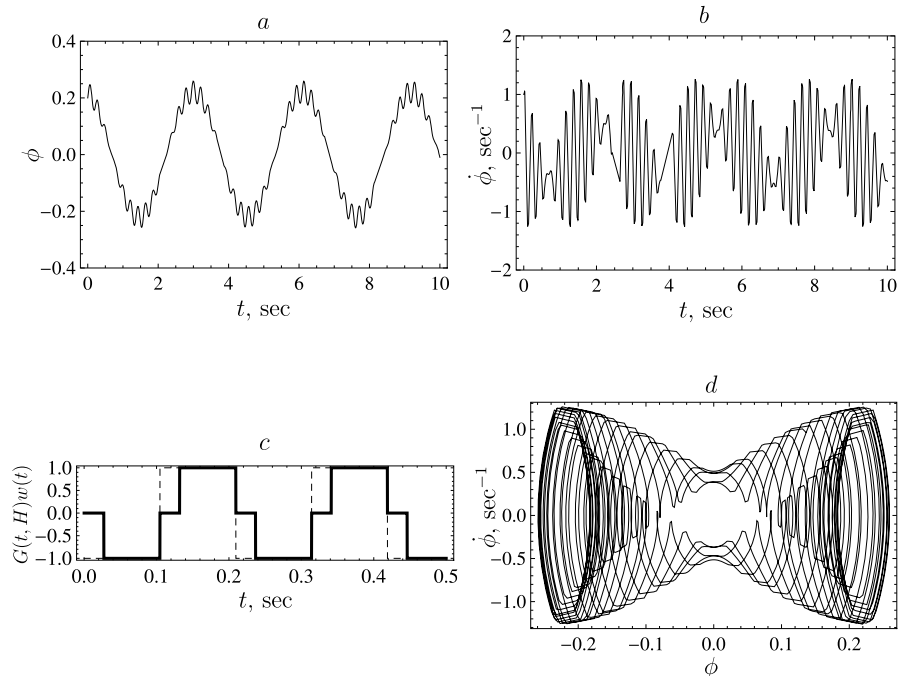


**Fig. 7** The dependence of the frequency  $\omega$  on the hysteretic parameter  $H$  (on the border of the stability zone, i.e., the condition  $|a_{11} + a_{22}| = 2$  takes place) for various  $a$ : *thin curve* is  $a = 0.1$  m, *thick curve* is  $a = 0.2$  m, *dashed curve* is  $a = 0.3$  m

**Fig. 8** Panels **a** and **b**: characteristics of the inverted pendulum described by Eq. (2) (modeling parameters are presented in the main text); panel **c**: the control function (*solid line* corresponds to hysteretic control, *dashed line* corresponds to the absence of the hysteretic control); panel **d**: phase portrait



This implies that the initial conditions satisfy the following expressions:

$$\phi_{10} = \frac{a_{12}}{a_{11} - 1} \phi_{20}, \quad \phi_{20} = \frac{a_{21}}{a_{22} - 1} \phi_{10}, \tag{18}$$

i.e., lie on a straight line  $z_1: \dot{\phi} = K_1\phi$ , where the coefficient  $K_1$  is

$$K_1 = \frac{a_{11} - 1}{a_{12}} = \frac{a_{21}}{a_{22} - 1}. \tag{19}$$

This equality ensures that the condition (15) is valid. If for the initial conditions  $(\phi_{10}, \phi_{20})$  can be found a pair of the parameters  $a$  and  $\omega$ , which lies on the border of the stability zone (at fixed  $H$ ) and satisfies Eq. (18) then this pair is unique. The opposite statement is also true.

In similar manner, we find that the periodic solutions with period  $T_2$  exist for initial conditions that satisfy the equations:

$$\phi_{10} = \frac{a_{12}}{1 + a_{11}} \phi_{20}, \quad \phi_{20} = \frac{a_{21}}{1 + a_{22}} \phi_{10}. \tag{20}$$

In an analogous manner, these initial conditions lie on a straight line  $z_2: \dot{\phi} = K_2\phi$  with the coefficient

$$K_2 = \frac{a_{11} + 1}{a_{12}} = \frac{a_{21}}{a_{22} + 1}. \tag{21}$$



Corresponding parameters  $a$  and  $\omega$  have been obtained from the numerical solution of Eqs. (19) and (21). Namely, for the solutions of Eq. (2) with the initial conditions that satisfy Eq. (19) the parameters  $a$  and  $\omega$  are  $a = 0.2$  m and  $\omega = 18.73$  s<sup>-1</sup> (hysteretic nonlinearity  $H = 0.05$  m). For the solutions with the initial conditions that satisfy Eq. (21), the corresponding parameters are  $a = 0.43$  m and  $\omega = 15.02$  s<sup>-1</sup> (at the same value of the hysteretic nonlinearity). However, the obtained periodic solutions (using the corresponding parameters  $a$  and  $\omega$ ) are not stable (in the strict sense). Therefore, the numerical simulation of these solutions cannot be made without a special regularization procedure.

However, we plot (see the Fig. 9) the surfaces in the space of parameters  $\omega$ ,  $a$ , and  $H$  that satisfy the existence conditions for the periodic solutions (Eqs. (19) and (21)). The complicated shape of the obtained surfaces is connected with the fact that the values of the parameters that determine the periodic solutions are placed on the boundary of the stability zone (see, e.g., Eqs. (10) and (11)) where the corresponding solutions are not stable. Moreover, the obtained surfaces (more specific, the dependencies that determine such surfaces) are the solutions of the essentially nonlinear equations (19) and (21) (the parameters  $a_{ij}$  in these equations are the elements of the monodromy matrix (9)).

## 6 Conclusions

In this paper, we have analyzed the inverted pendulum with the oscillating suspension point under hysteretic control (hysteretic nonlinearity) in the form of a backlash. More specific, the explicit condition for the stability of such a system has been obtained using the monodromy matrix technique (for the monodromy matrix is also obtained the explicit expression). The periodic solutions in such a system is also analyzed and the corresponding equations for the parameters  $a$  and  $\omega$  are obtained. Here, it should be pointed out that the dynamics of the inverted pendulum with hysteretic control qualitatively differs from the dynamics of the pendulum with conventional control. The presence of the hysteresis element complicates the study of the dynamics of mechanical systems. As a result, the main results of the presented paper were obtained using the numerical simulations only. It should be noted

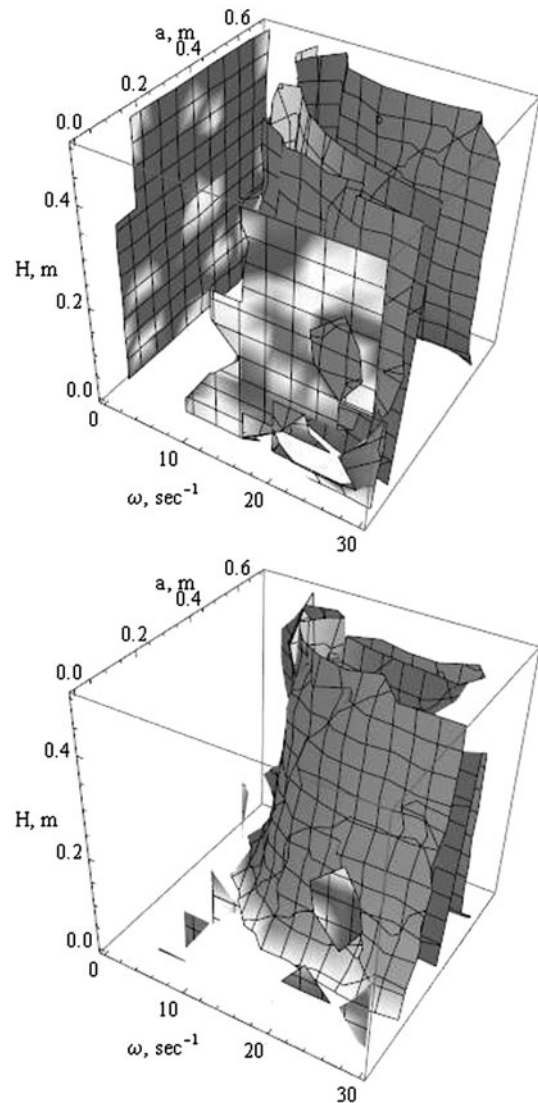


**Fig. 9** Surfaces in the space of parameters  $\omega$ ,  $a$ , and  $H$  that satisfy Eq. (19) (top panel) and Eq. (21) (bottom panel)

also that the same model can be used in the economics, namely for the problem of optimal production [30].

**Acknowledgements** This work is supported by the RFBR grants 11-08-00032-a, 12-07-00252-a, 13-08-00532-a.

## References

1. Arinstein, A., Gitterman, M.: Inverted spring pendulum driven by a periodic force: linear versus nonlinear analysis. *Eur. J. Phys.* **29**, 385–392 (2008)
2. Åström, K.J., Furuta, K.: Swinging up a pendulum by energy control. *Automatica* **36**, 287–295 (2000)

3. Bloch, A.M., Leonard, N.E., Marsden, J.E.: Controlled Lagrangians and the stabilization of mechanical systems. i. the first matching theorem. *IEEE Trans. Autom. Control* **45**, 2253–2270 (2000)
4. Boubaker, O.: The inverted pendulum: a fundamental benchmark in control theory and robotics. In: International Conference on Education and e-Learning Innovations (ICEELI 2012), pp. 1–6 (2012)
5. Butikov, E.I.: Subharmonic resonances of the parametrically driven pendulum. *J. Phys. A, Math. Theor.* **35**, 6209 (2002)
6. Butikov, E.I.: An improved criterion for Kapitza's pendulum stability. *J. Phys. A, Math. Theor.* **44**, 295,202 (2011)
7. Butikov, E.I.: Oscillations of a simple pendulum with extremely large amplitudes. *Eur. J. Phys.* **33**, 1555–1563 (2012)
8. Chang, L.H., Lee, A.C.: Design of nonlinear controller for bi-axial inverted pendulum system. *IET Control Theory Appl.* **1**, 979–986 (2007)
9. Chaturvedi, N.A., McClamroch, N.H., Bernstein, D.S.: Stabilization of a 3d axially symmetric pendulum. *Automatica* **44**, 2258–2265 (2008)
10. Chernous'ko, F.L., Reshmin, S.A.: Time-optimal swing-up feedback control of a pendulum. *Nonlinear Dyn.* **47**, 65–73 (2007)
11. Hasan, M., Saha, C., Rahman, M.M., Sarker, M.R.I., Aditya, S.K.: Balancing of an inverted pendulum using pd controller. *Dhaka Univ. J. Sci.* **60**, 115–120 (2012)
12. Henders, M., Soudack, A.: Dynamics and stability state-space of a controlled inverted pendulum. *Int. J. Non-Linear Mech.* **31**, 215–227 (1996)
13. Huang, J., Ding, F., Fukuda, T., Matsuno, T.: Modeling and velocity control for a novel narrow vehicle based on mobile wheeled inverted pendulum. *IEEE Trans. Control Syst. Technol.* **21**, 1607–1617 (2013)
14. Kapitza, P.L.: Dynamic stability of a pendulum when its point of suspension vibrates. *Sov. Phys. JETP* **21**, 588–592 (1951)
15. Kapitza, P.L.: Pendulum with a vibrating suspension. *Usp. Fiz. Nauk* **44**, 7–15 (1951) (in Russian)
16. Kim, K.D., Kumar, P.: Real-time middleware for networked control systems and application to an unstable system. *IEEE Trans. Control Syst. Technol.* **21**, 1898–1906 (2013)
17. Krasnosel'skii, M.A., Burd, V.S., Kolesov, J.S.: *Nonlinear Almost Periodic Oscillations*. Wiley, New York (1973)
18. Krasnosel'skii, M.A., Pokrovskii, A.V.: *Systems with Hysteresis*. Springer, Berlin (1989)
19. Li, G., Liu, X.: Dynamic characteristic prediction of inverted pendulum under the reduced-gravity space environments. *Acta Astronaut.* **67**, 596–604 (2010)
20. Lozano, R., Fantoni, I., Block, D.J.: Stabilization of the inverted pendulum around its homoclinic orbit. *Syst. Control Lett.* **40**, 197–204 (2000)
21. Magnus, K., Popp, K.A.: *Schwingungen: eine Einfuehrung in die physikalische Grundlagen und die theoretische Behandlung von Schwingungsproblemen*. Teubner, Basel (1997)
22. Mason, P., Broucke, M., Piccoli, B.: Time optimal swing-up of the planar pendulum. *IEEE Trans. Autom. Control* **53**, 1876–1886 (2008)
23. Mata, G.J., Pestana, E.: Effective Hamiltonian and dynamic stability of the inverted pendulum. *Eur. J. Phys.* **25**, 717 (2004)
24. Merkin, D.R.: *Introduction to the Theory of Stability*. Springer, New York (1997)
25. Nelepin, R.A. (ed.): *Methods of Investigation of Automatic Control Nonlinear Systems*. Nauka, Moscow (1975) (in Russian)
26. Pippard, A.B.: The inverted pendulum. *Eur. J. Phys.* **8**, 203 (1987)
27. Pliss, V.A.: *Nonlocal Problems of the Theory of Oscillations*. Academic Press, New York (1966)
28. Reshmin, S.A., Chernous'ko, F.L.: A time-optimal control synthesis for a nonlinear pendulum. *J. Comput. Syst. Sci. Int.* **46**, 9–18 (2007)
29. Sato, C.: Correction of stability curves in Hill–Meissner's equation. *Math. Comput.* **20**, 98–106 (1966)
30. Semenov, M.E., Grachikov, D.V., Mishin, M.Y., Shevlyakova, D.V.: Stabilization and control models of systems with hysteresis nonlinearities. *Eur. Res.* **20**, 523–528 (2012)
31. Sieber, J., Krauskopf, B.: Complex balancing motions of an inverted pendulum subject to delayed feedback control. *Physica D* **197**, 332–345 (2004)
32. Siuka, A., Schöberl, M.: Applications of energy based control methods for the inverted pendulum on a cart. *Robot. Auton. Syst.* **57**, 1012–1017 (2009)
33. Stephenson, A.: On an induced stability. *Philos. Mag.* **15**, 233 (1908)
34. Wang, J.J.: Simulation studies of inverted pendulum based on pid controllers. *Simul. Model. Pract. Theory* **19**, 440–449 (2011)
35. Yavin, Y.: Control of a rotary inverted pendulum. *Appl. Math. Lett.* **12**, 131–134 (1999)
36. Yue, J., Zhou, Z., Jiang, J., Liu, Y., Hu, D.: Balancing a simulated inverted pendulum through motor imagery: an eeg-based real-time control paradigm. *Neurosci. Lett.* **524**, 95–100 (2012)
37. Zhang, Y.X., Han, Z.J., Xu, G.Q.: Expansion of solution of an inverted pendulum system with time delay. *Appl. Math. Comput.* **217**, 6476–6489 (2011)